

Supplementary Materials: Performance of Solar-Induced Chlorophyll Fluorescence in Estimating Water-Use Efficiency in a Temperate Forest

Xiaoliang Lu ^{1,2}, Zhunqiao Liu ^{2,3}, Yuyu Zhou ⁴, Yaling Liu ⁵ and Jianwu Tang ^{2,*}

¹ Department of Forest Ecosystems and Society, Oregon State University, Corvallis, OR 97331, USA; luxiaoliangresearch@gmail.com

² The Ecosystems Center, Marine Biological Laboratory, Woods Hole, MA 02543, USA; liuzhunqiao@gmail.com

³ School of life sciences, Nanjing University, Xianlin Campus, 163 Xianlin Road, Nanjing, Jiangsu 210023, China

⁴ Department of Geological and Atmospheric Sciences, Iowa State University, Ames, IA 50011, USA; yuyuzhou@iastate.edu

⁵ Department of Earth and Environmental Engineering, Columbia University, 500 W. 120th St, 918 S. W. Mudd Hall, 500, New York, NY 10027, USA; yl3937@columbia.edu

* Corresponding: jtang@mbi.edu; Tel.: +1-508-289-7162

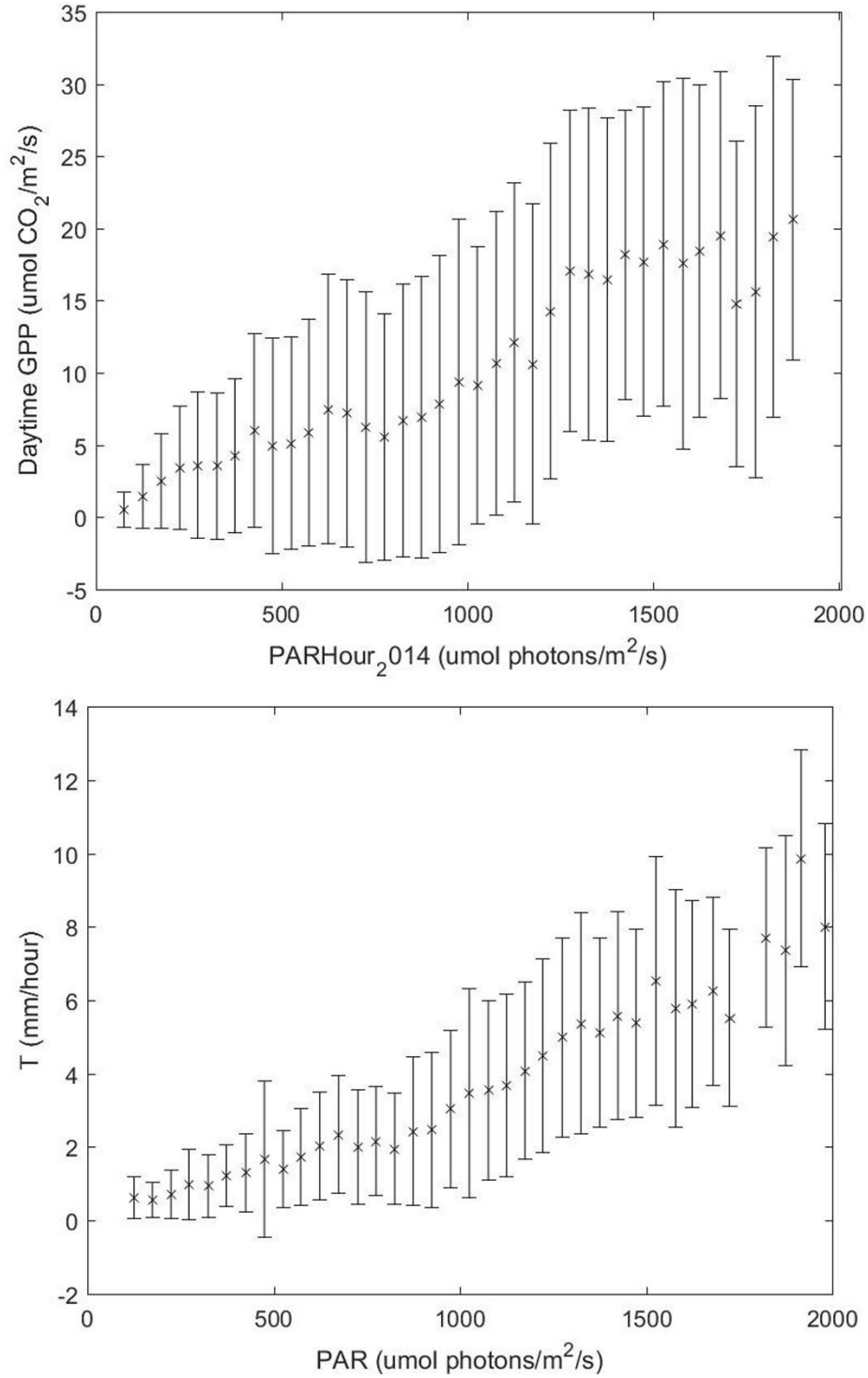


Figure S1. The responses of hourly daytime (a) gross primary production (GPP, umol CO₂ m/s) and (b) transpiration (T , mm/hour) to incident photosynthetically active radiation (PAR, $\mu\text{mol photons/m}^2/\text{s}$) during the growing season in 2014. The hourly ET time series was bin-averaged into 50 $\mu\text{mol photons/m}^2/\text{s}$ increment for PAR. Bars represent standard errors.

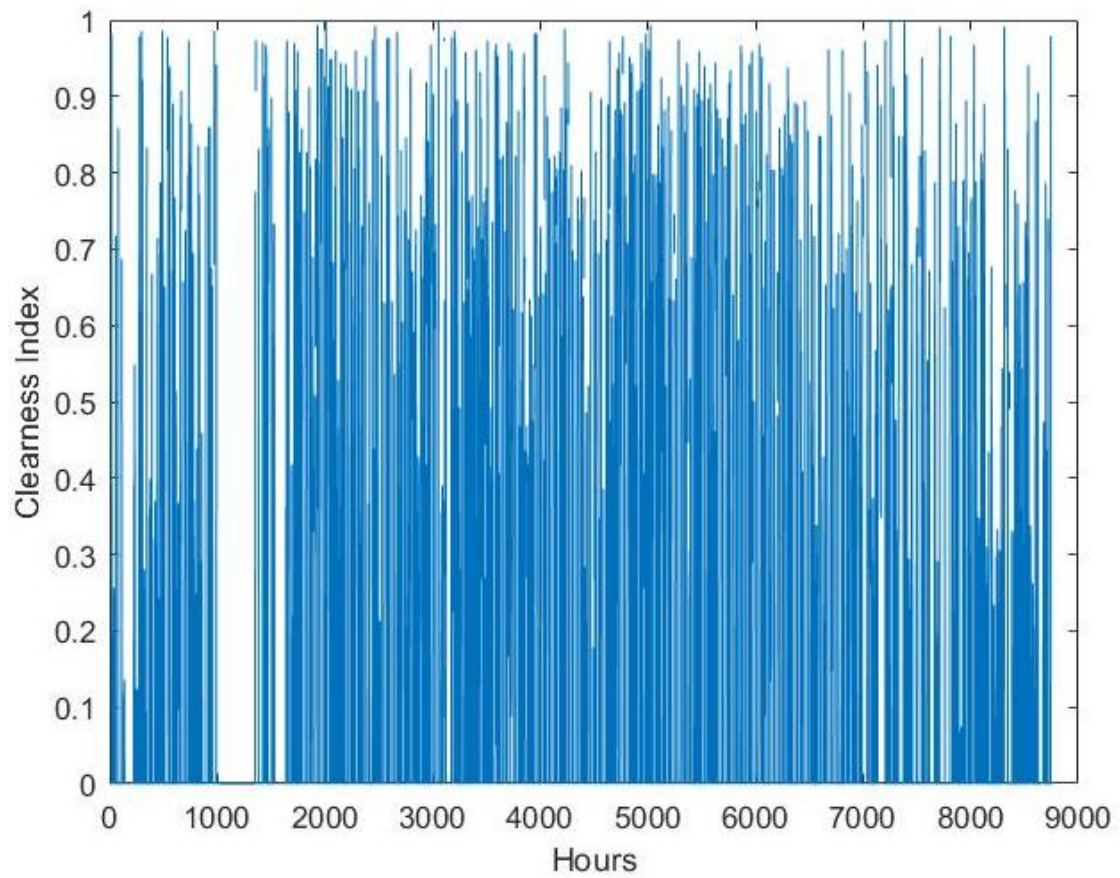


Figure S2. The hourly clearness index ([Gu et al., 1999](#)) at the Harvard site in 2014.

Table S1. The correlation coefficient (R^2) of the training and testing groups in predicting daily water use efficiency (WUE), intrinsic water use efficiency (WUE_i), inherent water use efficiency (IWUE) and underlying water use efficiency (uWUE) by using the linear regression analysis (LR) and Gaussian processes regression (GPR), respectively. The training group has 60% of all daily measurements and the test group has the rest. The R^2 estimated from the testing group are provided in the parentheses.

	WUE		WUE_i		IWUE		uWUE	
	LR	GPR	LR	GPR	LR	GPR	LR	GPR
SIF ₆₈₇	0.00 (0.00)	0.01 (0.00)	0.02 (0.01)	0.02 (0.01)	0.20 (0.16)	0.38 (0.33)	0.09 (0.06)	0.34 (0.32)
SIF ₇₂₀	0.13 (0.13)	0.39 (0.35)	0.31 (0.26)	0.30 (0.27)	0.48 (0.44)	0.53 (0.47)	0.42 (0.38)	0.41 (0.39)
SIF ₇₆₁	0.14 (0.11)	0.40 (0.38)	0.39 (0.35)	0.48 (0.43)	0.58 (0.55)	0.58 (0.51)	0.43 (0.39)	0.52 (0.48)
SIF ₇₂₀ , SIF ₇₆₁	0.15 (0.11)	0.50 (0.50)	0.48 (0.43)	0.48 (0.41)	0.60 (0.56)	0.60 (0.56)	0.50 (0.47)	0.58 (0.54)
SIF ₆₈₇ , SIF ₇₂₀ , SIF ₇₆₁	0.21 (0.18)	0.52 (0.47)	0.50 (0.46)	0.60 (0.55)	0.61 (0.58)	0.62 (0.57)	0.51 (0.44)	0.60 (0.52)

Retrieve SIF at the absorption lines

It is important to note that canopy-level radiance ($L(\lambda)$) at wavelength λ received by the spectrometer contains contributions from two sources including reflected solar energy ($r(\lambda) * \frac{I(\lambda)}{\pi}$) and upwelling SIF emission ($F(\lambda)$), that is:

$$L(\lambda) = r(\lambda) * \frac{I(\lambda)}{\pi} + F(\lambda) \quad (1)$$

where $I(\lambda)$ is down-welling incoming solar irradiance; both $L(\lambda)$ and $I(\lambda)$ are provided by the SIF observation system. At some absorption lines caused by either atmosphere absorption bands or the Fraunhofer lines, however, $r(\lambda)$ and $F(\lambda)$ can be represented by some mathematical functions (Zhao et al., 2014). Within the spectral range from 680 nm to 775 nm, there are three main absorption lines including O₂-B at 687 nm, water vapor at 720 nm and O₂-A at 761 nm (Table S2).

Table S2. The central wavelengths and spectral ranges of the absorption lines used for retrieving SIF emission.

Absorption lines	Central Wavelength (nm)	Spectral Range (nm)
O ₂ -B	687	683–692
Water vapor	720	714–722
O ₂ -A	761	757–771

Following the Spectral Fitting Method (SFM) proposed by Zhao et al (2014), we can express $r(\lambda)$ and $F(\lambda)$ by using the second order Taylor polynomials at these three lines (λ):

$$r(\lambda) = b_1 + b_2 * (\lambda - \lambda_c) + b_3 * (\lambda - \lambda_c)^2 \quad (2)$$

$$F(\lambda) = b_4 + b_5 * (\lambda - \lambda_c) + b_6 * (\lambda - \lambda_c)^2 \quad (3)$$

where λ_c are the central wavelengths of the absorption lines (Table S2). b_1, b_2, b_3, b_4, b_5 and b_6 are six unknown coefficients in the above two equations. Combining Eq. (1), (2) and (3), we have:

$$L(\lambda) = (\lambda - \lambda_c)^2 * \frac{I(\lambda)}{\pi} * b_6 + (\lambda - \lambda_c) * \frac{I(\lambda)}{\pi} * b_5 + \frac{I(\lambda)}{\pi} * b_4 + (\lambda - \lambda_c)^2 * b_3 + (\lambda - \lambda_c) * b_2 + b_1 \quad (4)$$

To separate $r(\lambda)$ and $F(\lambda)$ at a specific absorption line, one needs at least six measurements values of $L(\lambda)$ and $I(\lambda)$ within corresponding spectral range. After this step, we should have SIF emission at the three absorption lines named $F(687)$, $F(720)$ and $F(761)$ at each instantaneous time step.

Due to poor weather conditions such as scattered clouds and heavy rainfall, some $F(\lambda)$ may have negative values which were removed from the further analysis.

References

- Gu, L.H.; Fuentes, J.D.; Shugart, H.H.; Staebler, R.M.; Black, T.A. Responses of net ecosystem exchanges of carbon dioxide to changes in cloudiness: Results from two North American deciduous forests. *J. Geophys. Res.-Atmos.* **1999**, *104*, 31421-31434.
- Zhao, F.; Guo, Y.Q.; Verhoef, W.; Gu, X.F.; Liu, L.Y.; Yang, G.J. A method to reconstruct the solar-induced canopy fluorescence spectrum from hyperspectral measurements. *Remote Sensing* **2014**, *6*, 10171-10192.